12-5-2022

A Finite Difference Approach to Study the Impact of Boundary Conditions on the Acoustical Behavior of Particle Stacks

Zhuang Mo
Purdue University, mo26@purdue.edu

Guochenhao Song
Purdue University, song520@purdue.edu

Tongyang Shi
Institute of Acoustics, Chinese Academy of Sciences, shitongyang@mail.ioa.ac.cn

J Stuart Bolton
Purdue University, bolton@purdue.edu

A FINITE DIFFERENCE APPROACH TO STUDY THE IMPACT OF BOUNDARY CONDITIONS ON THE ACOUSTICAL BEHAVIOR OF PARTICLE STACKS

Zhuang Mo, Guochenhao Song, Tongyang Shi, J. Stuart Bolton

PURDUE UNIVERSITY | Ray W. Herrick Laboratories

Content

- Background
- Finite Difference Approach
- Testing Results
- Conclusions

Background

https://www.3m.com/3M/en_US/p/d/b40064606/

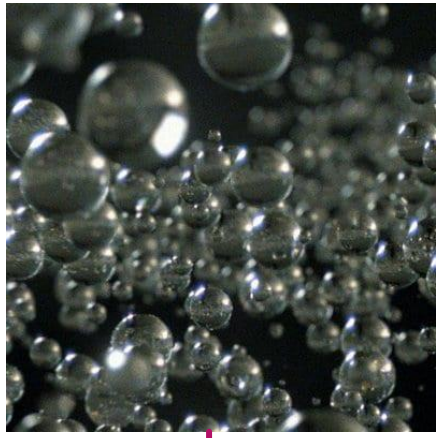

Glass bubbles

The measured results are from stacks of 3M™ Glass Bubbles K20, which has particle radius of $30\ \mu m$ (stack bulk density $125.4\ kg/m^3$, porosity 0.373).

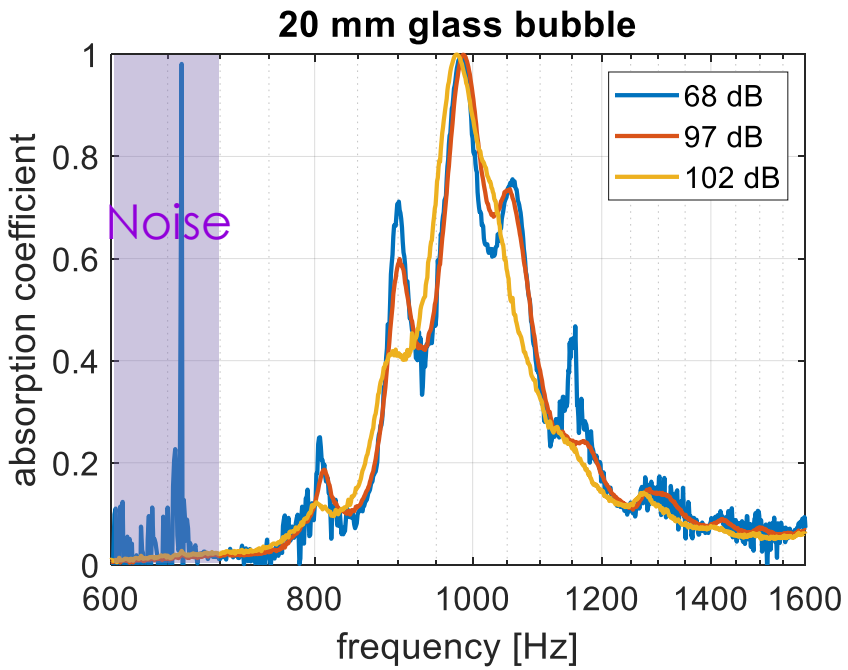

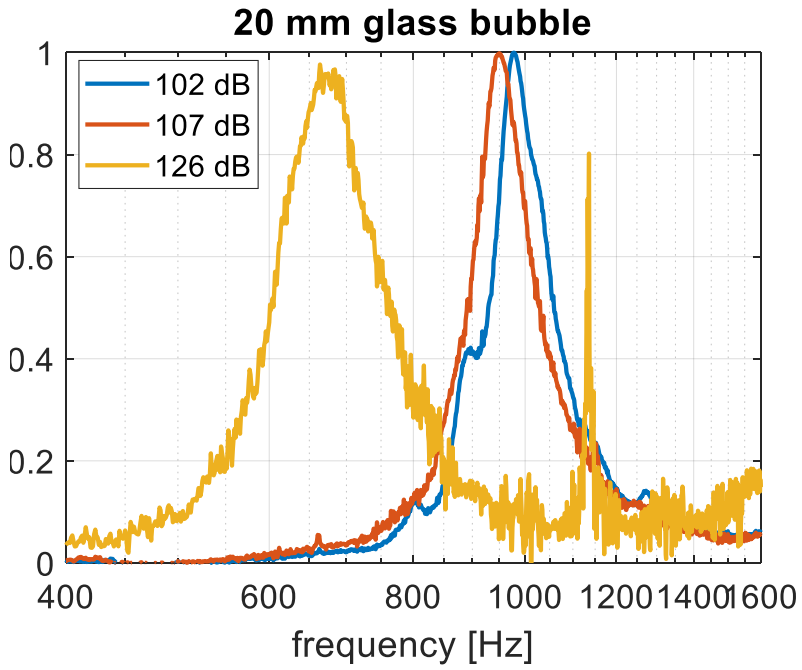

- Under low input level, the bubble stacks show modal response
- The change of behavior happens at approximately 100 dB input
- Under higher input level, the response is more fluid-like

Finite Difference Approach

Following the theory proposed by Biot (Biot, 1956):

$$\begin{bmatrix}\sigma_x\\ \sigma_y\\ \sigma_z\\ \tau_x\\ \tau_y\\ \tau_z\\ s\end{bmatrix} = \begin{bmatrix}P & & & & & & Q\\ & P & & & & & Q\\ & & P & & & & Q\\ & & & N & & & \\ & & & & N & & \\ & & & & & N & \\ Q & Q & Q & & & & R\end{bmatrix}\begin{bmatrix}e_x\\ e_y\\ e_z\\ \gamma_x\\ \gamma_y\\ \gamma_z\\ \epsilon\end{bmatrix}$$

Equations of motion

$$\nabla \cdot \underline{\underline{\boldsymbol{\sigma}}} = \rho_{11}\ddot{\underline{\mathbf{u}}} + \rho_{12}\ddot{\underline{\mathbf{U}}}$$
$$\nabla \cdot s = \rho_{12}\ddot{\underline{\mathbf{u}}} + \rho_{22}\ddot{\underline{\mathbf{U}}}$$

Linear system, harmonic excitation, Viscous dissipation

$$\nabla \cdot \underline{\underline{\boldsymbol{\sigma}}} = -\omega^2\left(\tilde{\rho}_{11}\underline{\mathbf{u}} + \tilde{\rho}_{12}\underline{\mathbf{U}}\right)$$
$$\nabla \cdot s = -\omega^2\left(\tilde{\rho}_{12}\underline{\mathbf{u}} + \tilde{\rho}_{22}\underline{\mathbf{U}}\right)$$

- The solid phase stresses are not only depending on solid phase strains but also fluid dilatation
- The fluid phase load, $s = -\phi p$, depends not only on the fluid dilatation but also solid phase expansion

Not convenient to consider fluid phase displacement on different directions separately

Finite Difference Approach

$$\nabla \cdot \underline{\underline{\boldsymbol{\sigma}}} = -\omega^2\left(\tilde{\rho}_{11}\underline{\mathbf{u}} + \tilde{\rho}_{12}\underline{\mathbf{U}}\right)$$
$$\nabla \cdot s = -\omega^2\left(\tilde{\rho}_{12}\underline{\mathbf{u}} + \tilde{\rho}_{22}\underline{\mathbf{U}}\right)$$

U-P formulation
Atalla et al., 1998

$$\nabla \cdot \underline{\underline{\hat{\boldsymbol{\sigma}}}}^s + \omega^2\tilde{\rho}\underline{\mathbf{u}} + \tilde{\gamma}\nabla p = 0$$
$$\nabla^2 p + \omega^2\frac{\tilde{\rho}_{22}}{R}p - \omega^2\frac{\tilde{\rho}_{22}}{\phi^2}\tilde{\gamma}\,\nabla \cdot \underline{\mathbf{u}} = 0$$

The *in vacuo* stress tensor is defined as:

$$\underline{\underline{\hat{\boldsymbol{\sigma}}}}^s = \left(K_b - \frac{2}{3}N\right)\nabla \cdot \underline{\mathbf{u}} \cdot \underline{\underline{\mathbf{I}}} + 2N\underline{\underline{\boldsymbol{\varepsilon}}}^s$$

Its relationship with the original solid stress tensor is:

$$\underline{\underline{\hat{\boldsymbol{\sigma}}}}^s = \underline{\underline{\boldsymbol{\sigma}}} + \phi\frac{Q}{R}p \cdot \underline{\underline{\mathbf{I}}} = \underline{\underline{\boldsymbol{\sigma}}} - \frac{Q}{R}s \cdot \underline{\underline{\mathbf{I}}}$$

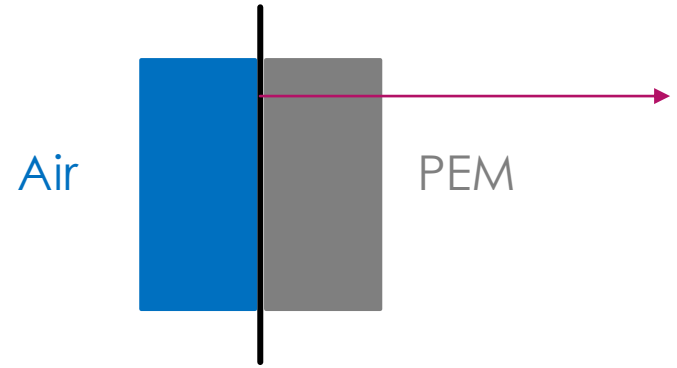

On interface:
$\underline{\underline{\hat{\boldsymbol{\sigma}}}}^s = \underline{\underline{\mathbf{0}}}$

Finite Difference Approach

Jassen's model – Force deflection in cylindrical container and friction on container wall (Duran, 2000, Springer)

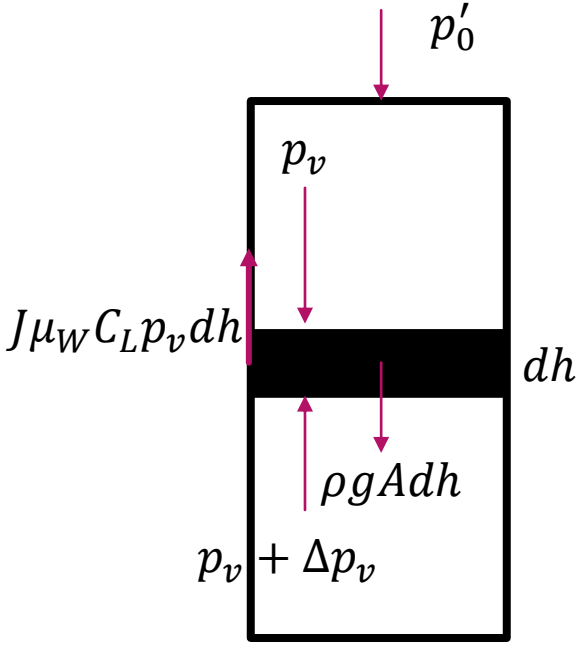

$$A\Delta p_v + J\mu_W C_L p_v dh = \rho g A dh$$

$$p_v = \frac{\rho g}{\beta}\left(1 - e^{-\beta x}\right) + p_0' e^{-\beta x}$$

β is the Jassen factor:

$$\beta = 4J\mu_W / d$$

For equilibrium status we use $p_0' = \rho_b g \cdot 2r_p$ to avoid zero stiffness at surface

Hertzian contact – effective stiffness increases with the contact surface area (Fischer-Cripps, 1999)

$$E = E_0 \sigma^{1/3}$$

With Jassen's model and Hertzian contact theory, the stiffness of particle stack can be expressed as a function of depth, which has been applied in previous studies, e.g., Matchett and Yanagida, 2003; Tsuruha et al., 2020

$$E = E_0 \left[\frac{\rho g}{\beta}\left(1 - e^{-\beta x}\right) + p_0' e^{-\beta x}\right]^{1/3}$$

$$\frac{\partial E}{\partial x} = \frac{1}{3} E_0 \left[\frac{\rho g}{\beta}\left(1 - e^{-\beta x}\right) + p_0' e^{-\beta x}\right]^{-2/3} (\rho g - \beta p_0') e^{-\beta x}$$

Finite Difference Approach

The fluid model is selected considering the spherical geometry of the particles. The viscous and thermal permeability, k_p and k_p' can be obtained according to (Boutin and Geindreau, 2008; Boutin and Geindreau, 2010; Venegas and Umnova, 2016):

$$k_p = -j\delta_v^2\left(1 - 3C/x^2\right)^{-1}$$

$$k_p' = -j\delta_t^2\left(1 - \zeta^3 + \frac{3\zeta}{x_t^2}\left(\zeta x_t \frac{1 + x_t + \tanh\left(x_t(\zeta - 1)\right)}{x_t + \tanh\left(x_t(\zeta - 1)\right)}\right) - 1\right)$$

where $\zeta = (1 - \phi)^{1/3}$, and all other parameters follow the definitions in the references. Hence, the fluid phase bulk modulus and wavenumber can be calculated:

$$K_{eq} = \frac{\gamma P_0}{\phi}\left(\gamma - j\omega\rho_0 \mathrm{Pr}(\gamma - 1)\frac{k_p'}{\phi\eta}\right)^{-1}$$

$$k_{eq} = \omega\sqrt{\eta/j\omega k_p K_{eq}}$$

Finite Difference Approach

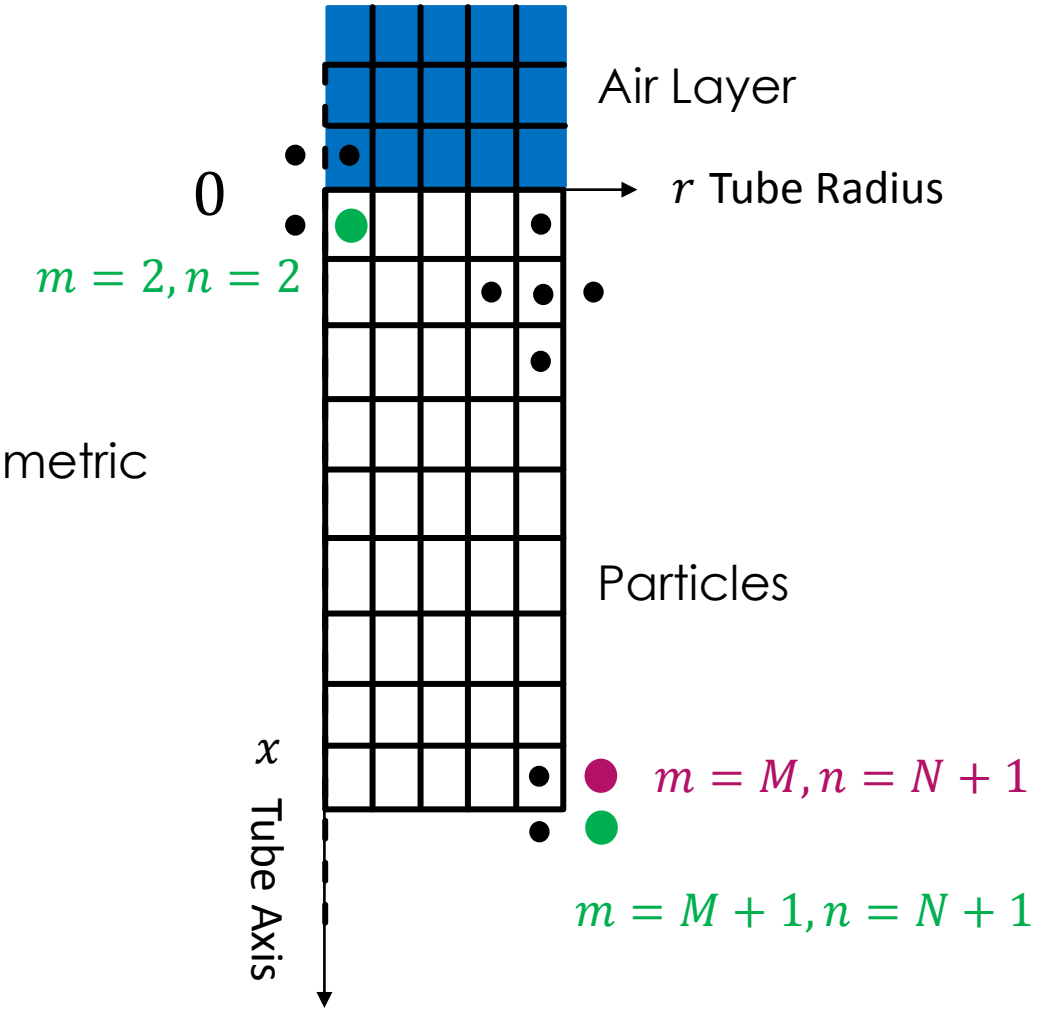

For inner nodes there are,

$$\left.\frac{\partial f}{\partial x}\right|_{m,n} = \frac{f_{m+1,n} - f_{m-1,n}}{2\Delta x}$$

$$\left.\frac{\partial f}{\partial r}\right|_{m,n} = \frac{f_{m,n+1} - f_{m,n-1}}{2\Delta r}$$

$$\left.\frac{\partial^2 f}{\partial x^2}\right|_{m,n} = \frac{f_{m+1,n} - 2f_{m,n} + f_{m-1,n}}{\Delta x^2}$$

$$\left.\frac{\partial^2 f}{\partial r^2}\right|_{m,n} = \frac{f_{m,n+1} - 2f_{m,n} + f_{m,n-1}}{\Delta r^2}$$

$$\left.\frac{\partial^2 f}{\partial x \partial r}\right|_{m,n} = \frac{f_{m+1,n+1} - f_{m-1,n+1} - f_{m+1,n-1} + f_{m-1,n-1}}{4\Delta x \Delta r}$$

Finite Difference Approach

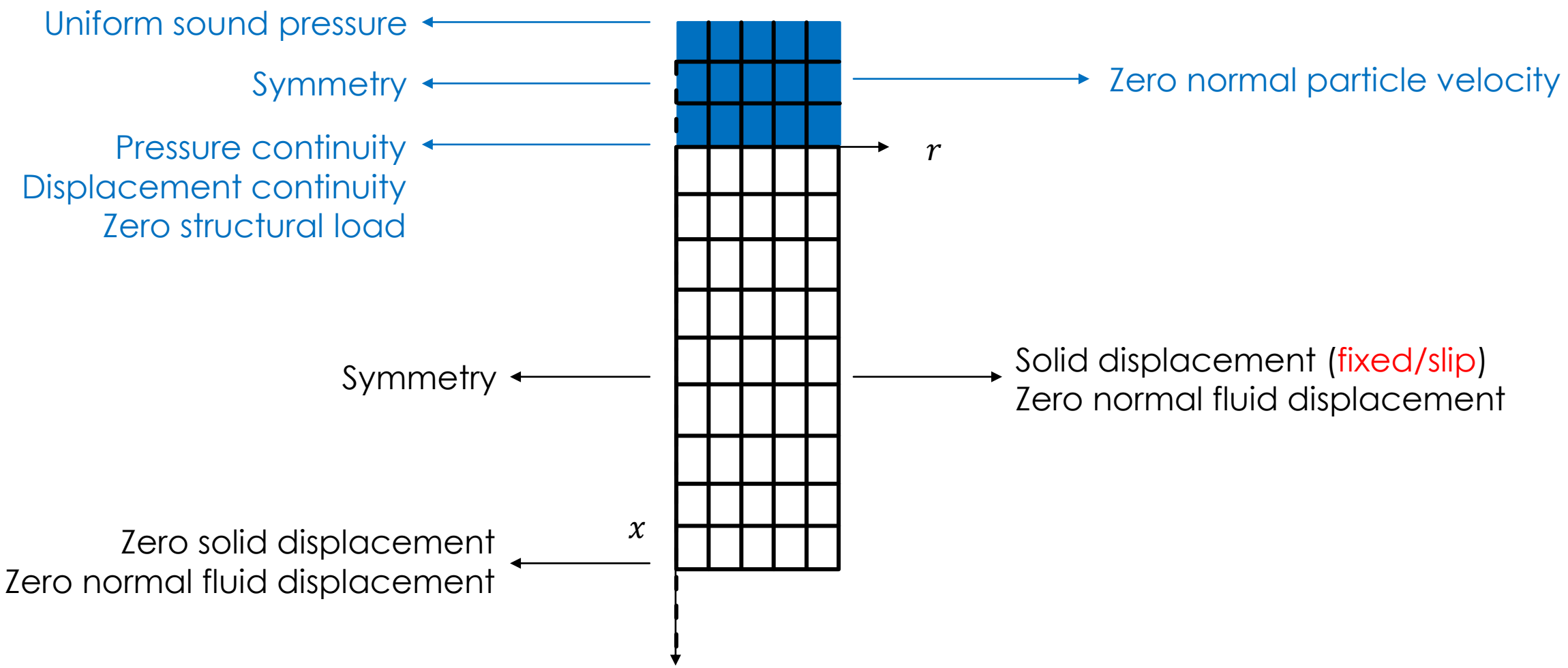

Finite Difference Approach

Slip boundary condition:

$$\left.\frac{\partial u^x}{\partial r}\right|_{r=R} = 0, u^r\Big|_{r=R} = 0$$

Fixed solid displacement:

$$u^x\Big|_{r=R} = 0, u^r\Big|_{r=R} = 0$$

If the slip boundary condition is applied all along the wall, the response will be purely 1D, which is equivalent to an infinite layer.
If the fixed boundary condition is applied, the response will be 2D.

20-mm-thick glass bubble simulation Varying stiffness achieved with 20 layers in analytical model (Dazel et al., 2013)

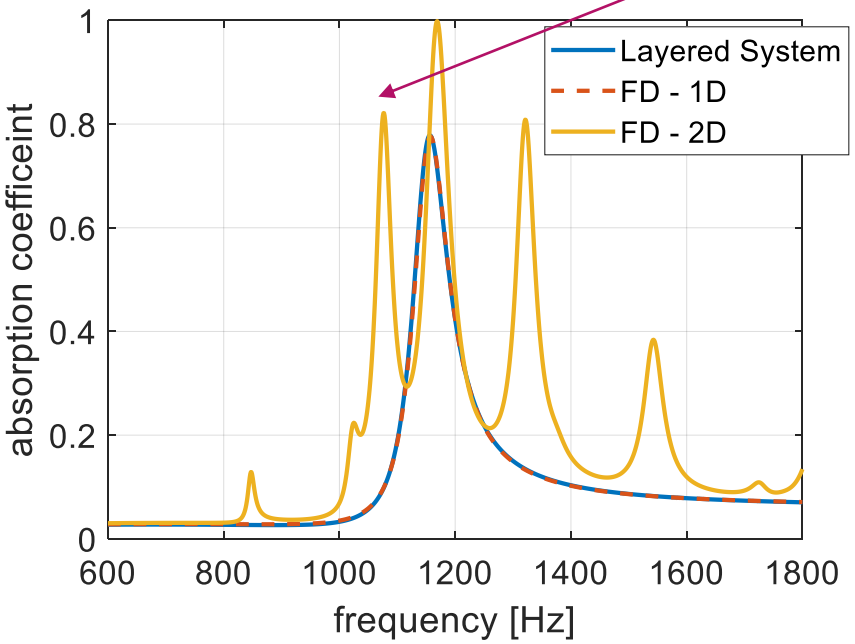

2D response with totally fixed solid phase on the wall at 1077 Hz.

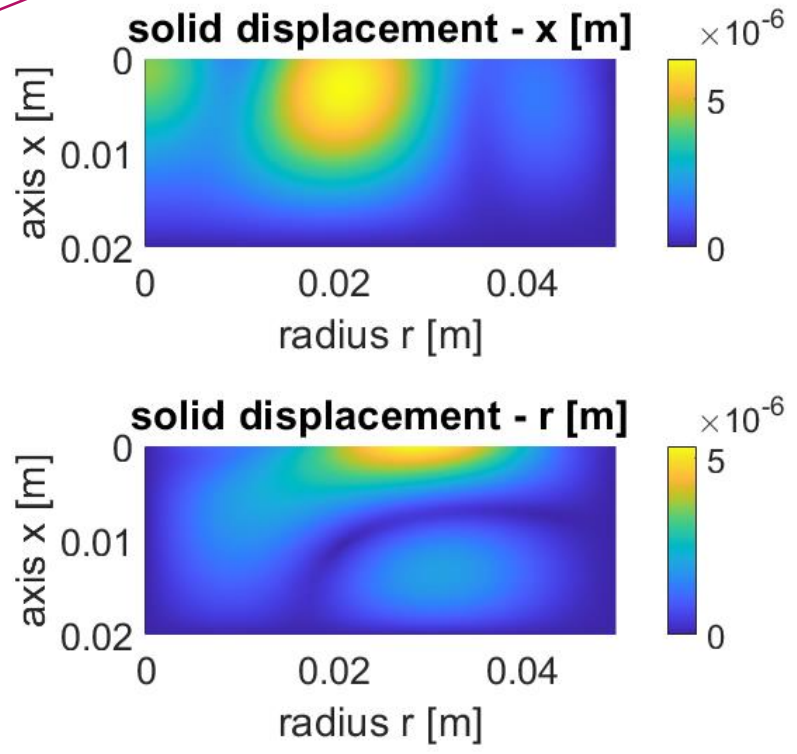

Testing Results

Mixed boundary condition:

$$\left.\frac{\partial u^x}{\partial r}\right|_{r=R} = 0 \ (m < m_d)$$

$$\left. u^x \right|_{r=R} = 0 \ (m \geq m_d)$$

m_d is the row number before which slip boundary condition is applied, and after which fixed boundary condition is applied.

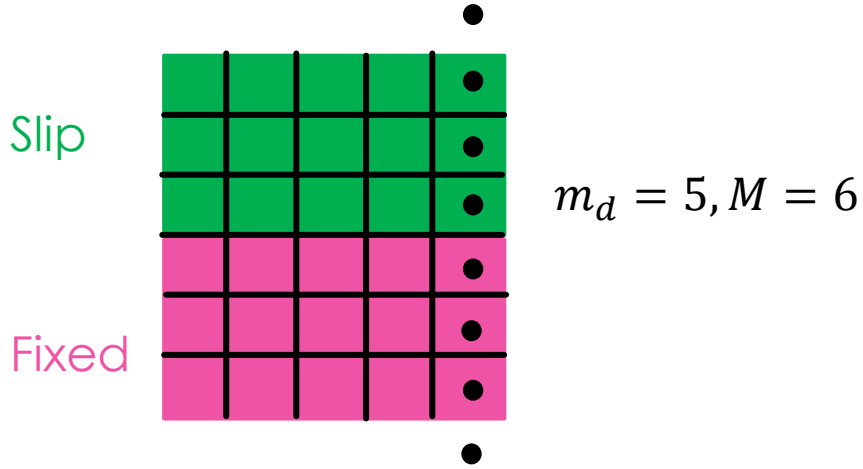

For simulations of 20-mm-thick glass bubble stacks, $M = 40$.

Testing Results – Low Input Level

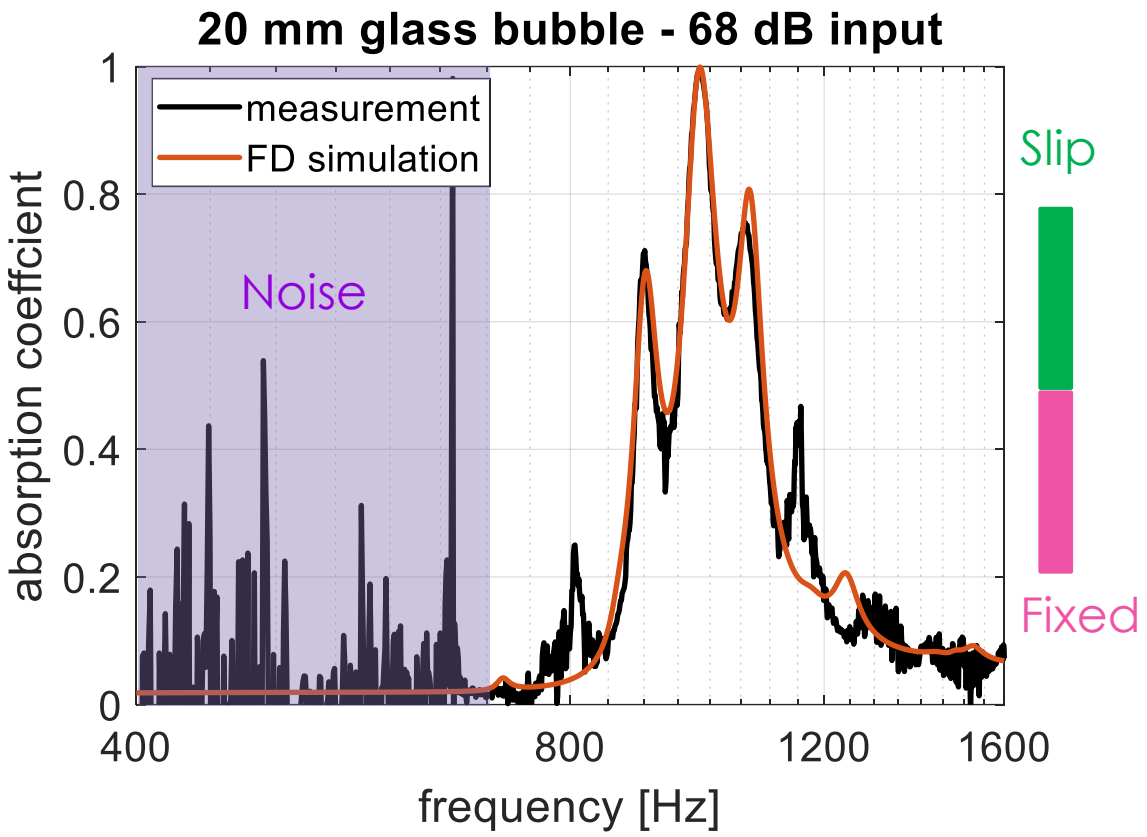

$E_0 = 1.45 \times 10^5$ Pa, $\nu = 0.29, \eta = 0.018$
$\beta = 18\ \mathrm{m}^{-1}, \boldsymbol{m_d = 20}$

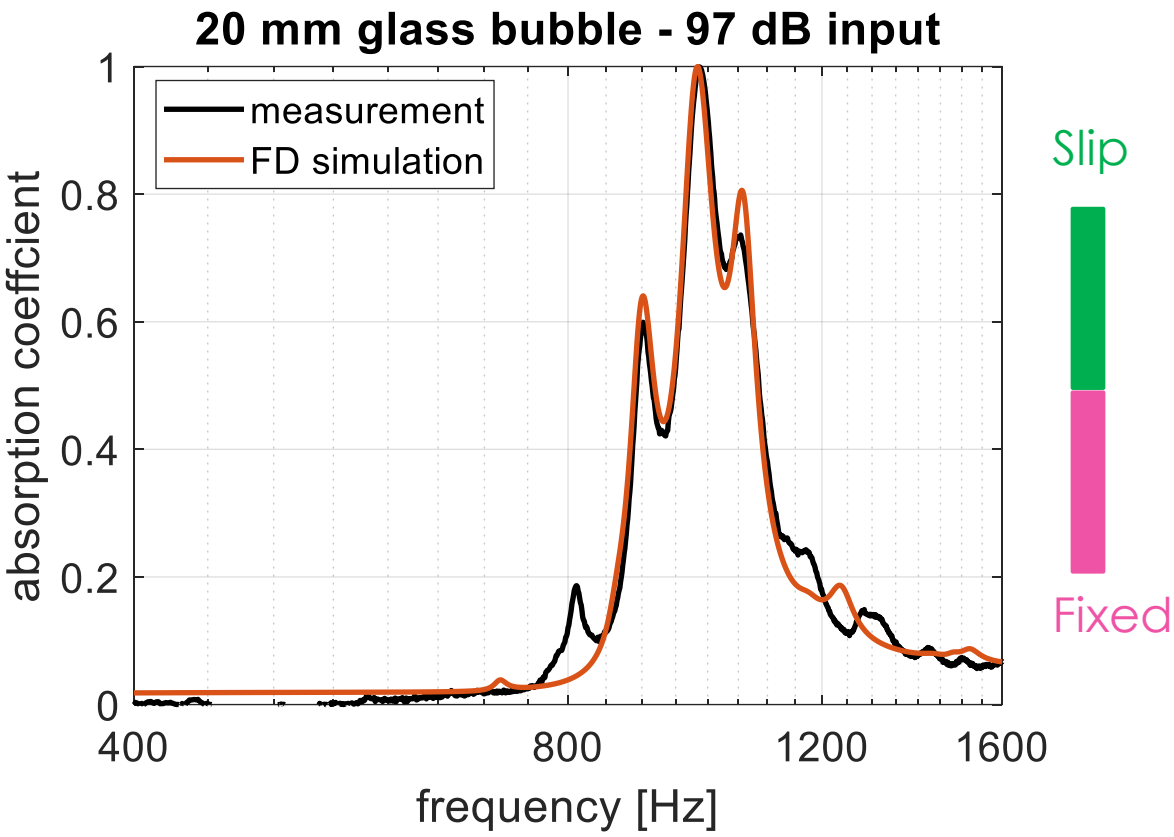

$E_0 = 1.45 \times 10^5$ Pa, $\nu = 0.29, \eta = 0.018$
$\beta = 18\ \mathrm{m}^{-1}, \boldsymbol{m_d = 21}$

Testing Results – Transition

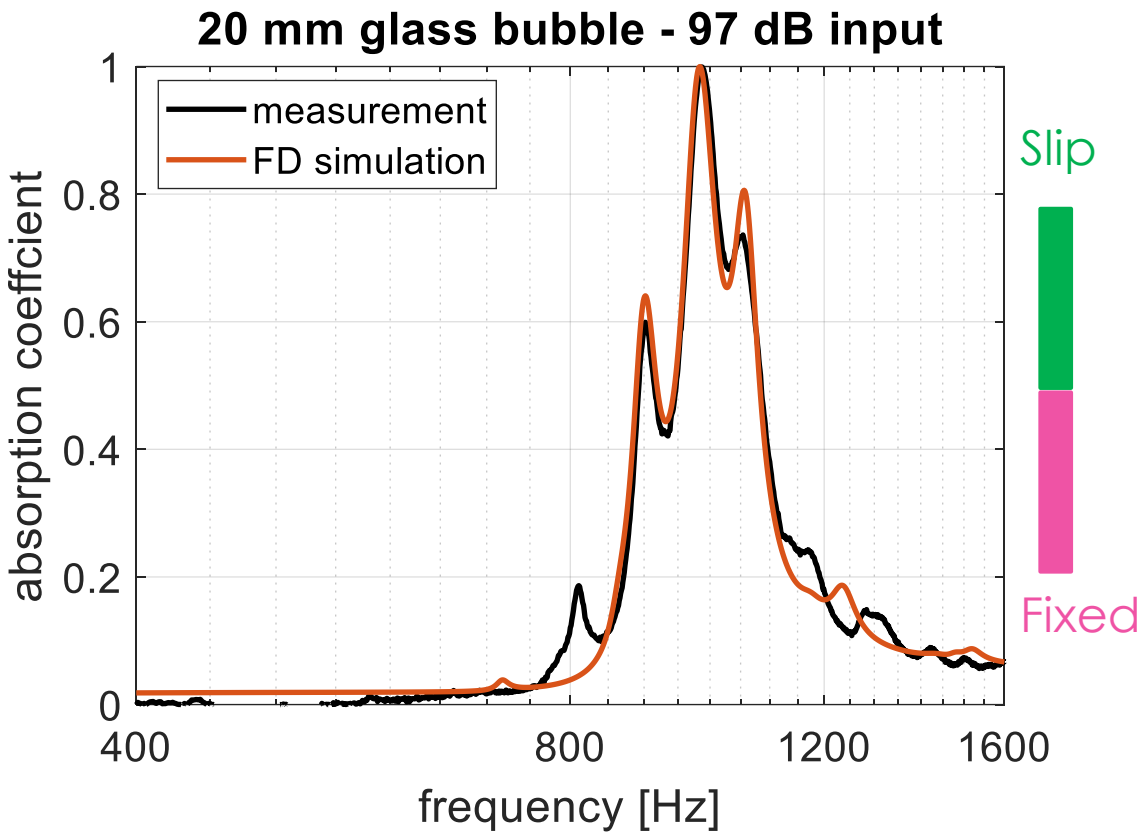

$E_0 = 1.45 \times 10^5$ Pa, $\nu = 0.29$, $\boldsymbol{\eta = 0.018}$
$\beta = 18\ \mathrm{m}^{-1}$, $\boldsymbol{m_d = 21}$

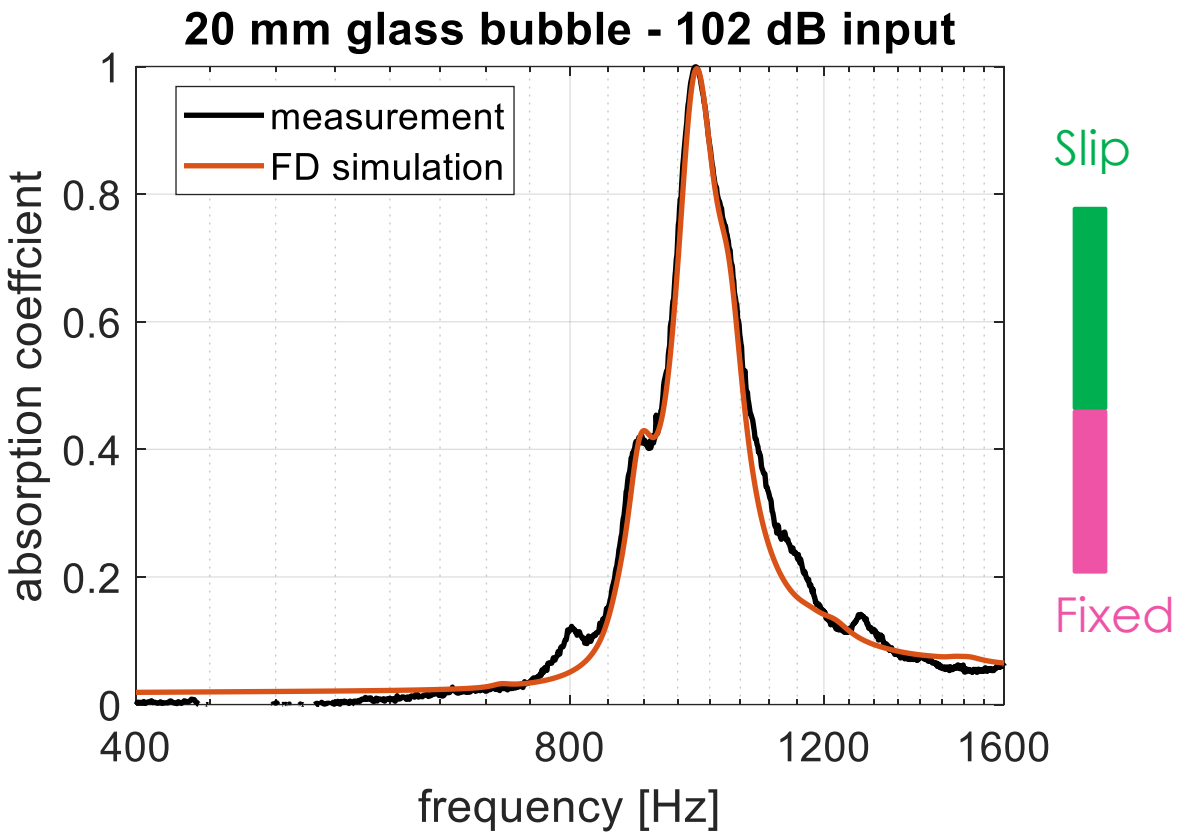

$E_0 = 1.45 \times 10^5$ Pa, $\nu = 0.29$, $\boldsymbol{\eta = 0.03}$
$\beta = 18\ \mathrm{m}^{-1}$, $\boldsymbol{m_d = 25}$

Testing Results – Transition

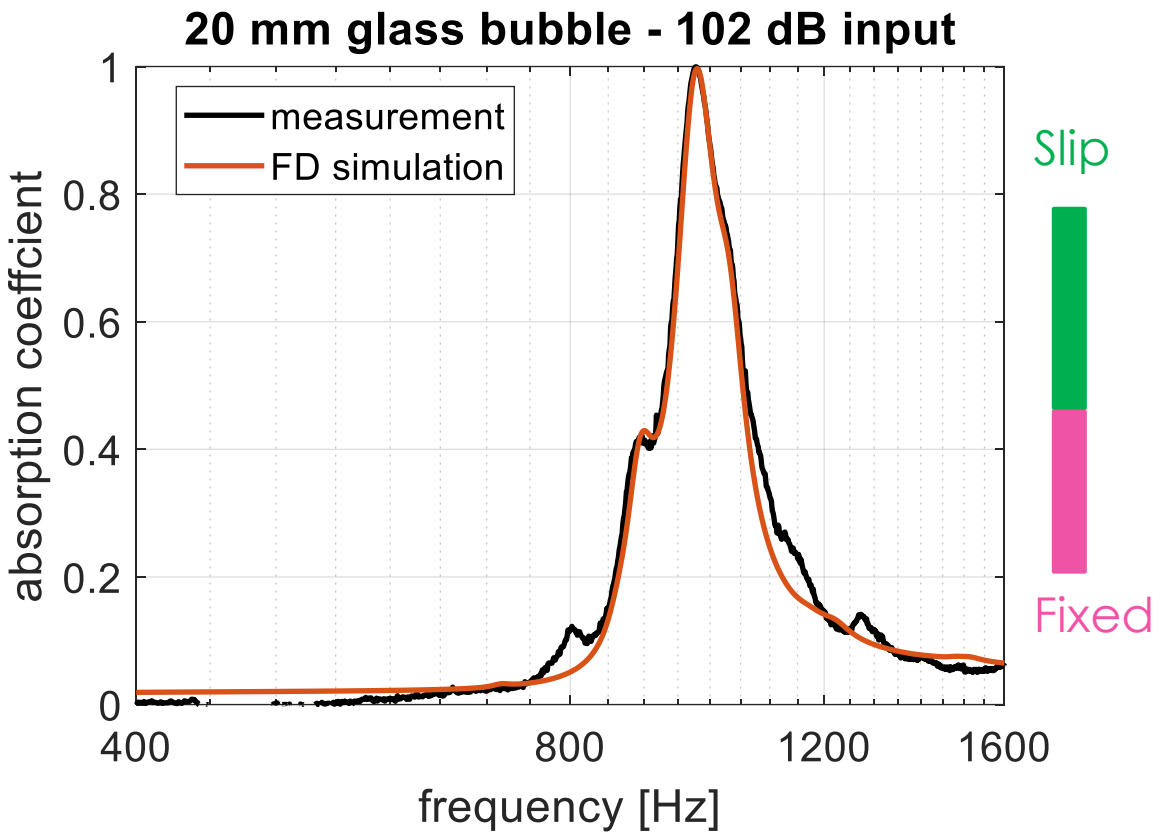

$E_0 = 1.45 \times 10^5$ Pa, $\nu = 0.29$, $\boldsymbol{\eta = 0.03}$
$\beta = 18\ \mathrm{m}^{-1}$, $\boldsymbol{m_d = 25}$

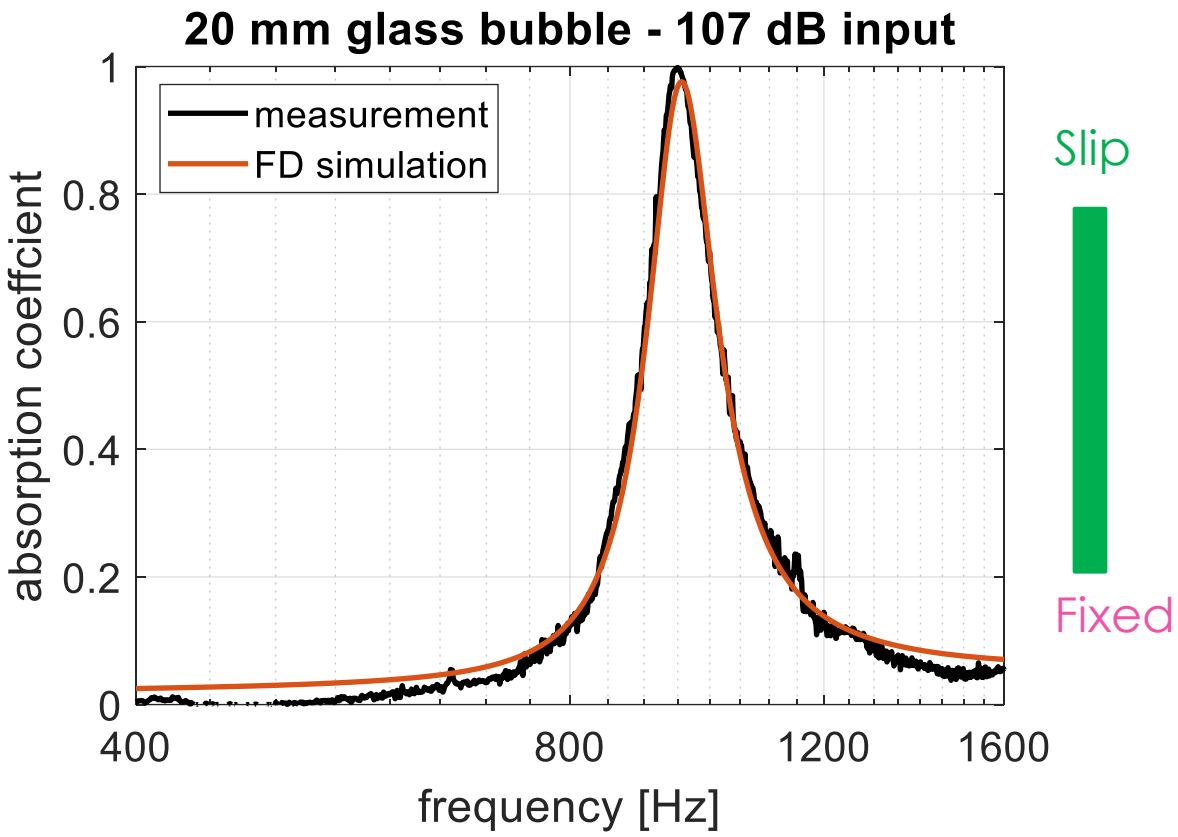

$E_0 = 1.45 \times 10^5$ Pa, $\nu = 0.29$, $\boldsymbol{\eta = 0.1}$
$\beta = 18\ \mathrm{m}^{-1}$, $\boldsymbol{m_d = 42}$

Testing Results – High Input Level

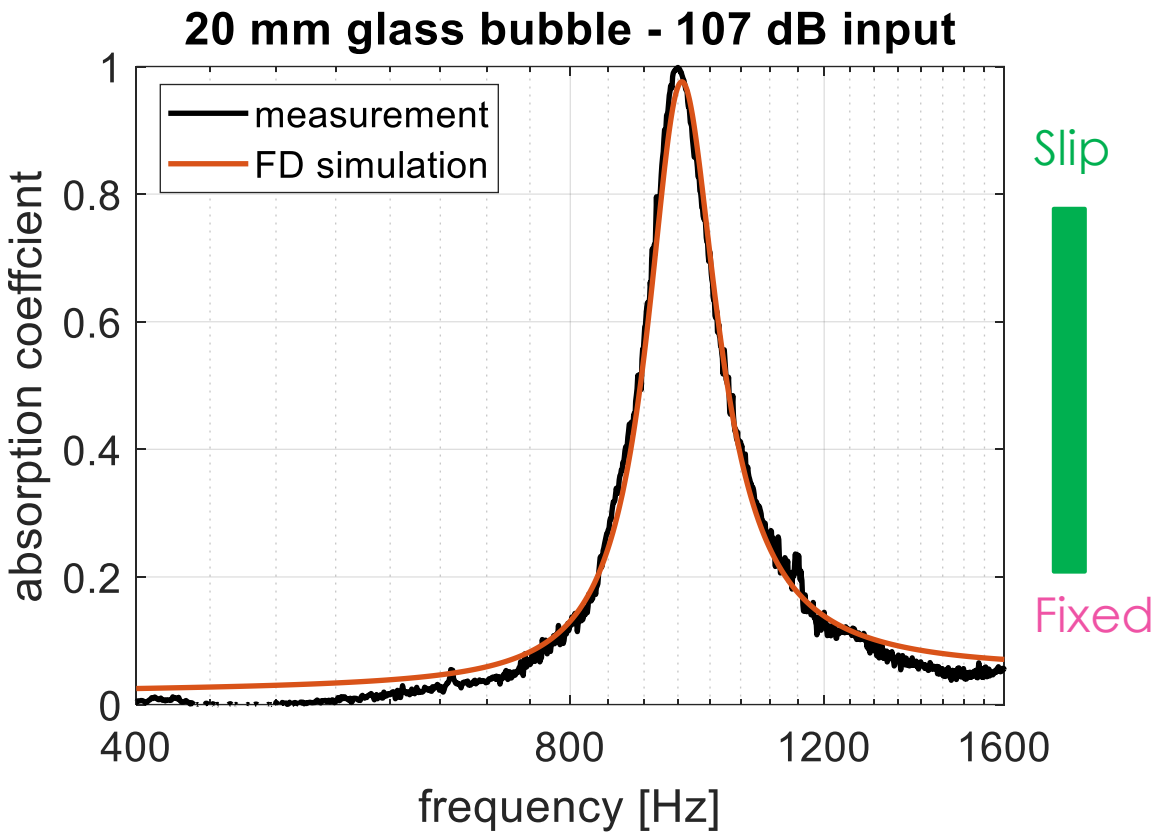

$E_0 = 1.45 \times 10^5$ Pa, $\nu = 0.29$, $\eta = 0.1$
$\beta = 18\ \mathrm{m}^{-1}$, $m_d = 42$

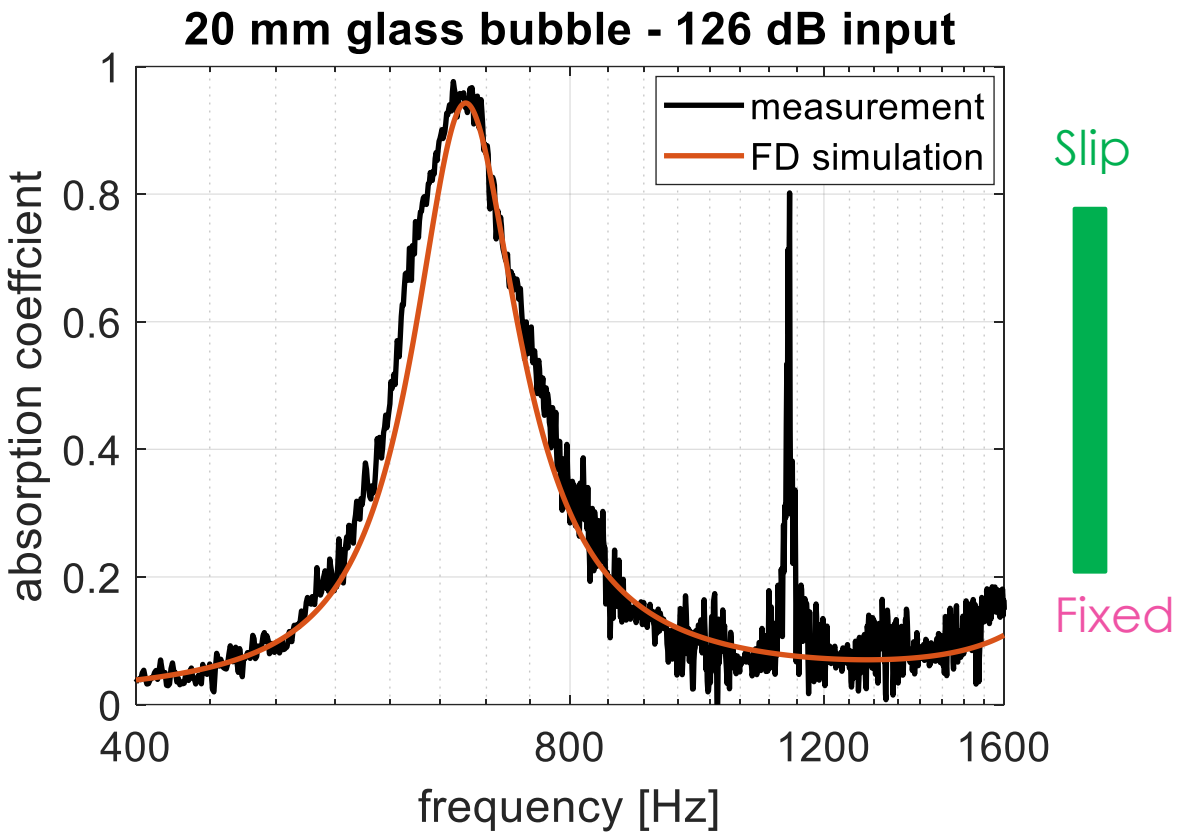

$E_0 = 3 \times 10^4$ Pa, $\nu = 0.29$, $\eta = 0.32$
$\beta = 18\ \mathrm{m}^{-1}$, $m_d = 42$

Conclusions

- A finite difference approach is developed
  - This approach is based on Biot theory, and incorporated Jassen's model and Hertzian contact theory to account for the stiffness variation in particle stacks
  - This approach is developed in cylindrical coordinates, align with realistic testing conditions. It also provides flexibility to apply different boundary conditions
  - Close match between FD simulation and acoustic measurement of glass bubbles can be achieved by adjusting model parameters, providing potential explanation of the behavior change of glass bubble stacks under different input levels.
- Future works
  - Incorporate more complete constitutive relations into the FD approach, so we can better predict the glass bubble behavior
  - Extend the approach to simulate measurement under different settings and of different particles

References

[1] Maurice A Biot. Theory of propagation of elastic waves in a fluid-saturated porous solid. i. low-frequency range. ii. higher frequency range. *The Journal of the Acoustical Society of America*, 28(2):168–191, 1956.

[2] Jean-François Allard and Noureddine Atalla. *Propagation of Sound in Porous Media: Modelling Sound Absorbing Materials, second edition*. John Wiley & Sons, 2009.

[3] Olivier Dazel, J.-P. Groby, B Brouard, and Catherine Potel. A stable method to model the acoustic response of multilayered structures. *Journal of Applied Physics*, 113(8):083506, 2013.

[4] Yeon June Kang, Bryce K Gardner, and J. Stuart Bolton. An axisymmetric poroelastic finite element formulation. *The Journal of the Acoustical Society of America*, 106(2):565–574, 1999.

[5] Rodolfo Venegas and Olga Umnova. Influence of sorption on sound propagation in granular activated carbon. *The Journal of the Acoustical Society of America*, 140(2):755–766, 2016.

[6] Takumasa Tsuruha, Yoshinari Yamada, Makoto Otani, and Yasushi Takano. Effect of casing on sound absorption characteristics of fine spherical granular material. *The Journal of the Acoustical Society of America*, 147(5):3418–3428, 2020.

[7] Andrew J. Matchett and Takeshi Yanagida. Elastic modulus of powder beds—the effects of wall friction: a model compared to experimental data. *Powder technology*, 137(3):148–158, 2003.

[8] Jacques Duran. *Sands, Powders, and Grains: An Introduction to the Physics of Granular Materials*. Springer, 2000.

[9] Francois-Xavier Bécot and Luc Jaouen. An alternative Biot's formulation for dissipative porous media with skeleton deformation. *The Journal of the Acoustical Society of America*, 134(6):4801–4807, 2013.

[10] Rodolfo Venegas, Claude Boutin, and Olga Umnova. Acoustics of multiscale sorptive porous materials. *Physics of Fluids*, 29(8):082006, 2017.

References

[11] George B Arfken, Hans J Weber, and Frank E Harris. *Mathematical Methods for Physicists: A Comprehensive Guide, seventh edition*. Elsevier, 2011.

[12] Anthony Fischer-Cripps. The hertzian contact surface. *Journal of materials science*, vol. 34, no. 1, pp. 129–137, 1999.

[13] Takumasa Tsuruha, Makoto Otani, and Yasushi Takano. Effect of acoustically-induced elastic softening on sound absorption coefficient of hollow glass beads with inner closed cavities. *The Journal of the Acoustical Society of America*, vol. 150, no. 2, pp. 841–850, 2021.

[14] Noureddine Atalla, Raymond Panneton, and Patricia Debergue. A mixed displacement-pressure formulation for poroelastic materials. *The Journal of the Acoustical Society of America*, vol. 104, no. 3, pp. 1444–1452, 1998.

[15] Claude Boutin and Christian Geindreau. Estimates and bounds of dynamic permeability of granular media. *The Journal of the Acoustical Society of America*, vol. 124, no. 6, pp. 3576–3593, 2008.

[16] Claude Boutin and Christian Geindreau. Periodic homogenization and consistent estimates of transport parameters through sphere and polyhedron packings in the whole porosity range. *Physical review E*, vol. 82, no. 3, p. 036 313, 2010.

[17] Zhuang Mo, Guochenhao Song, and J. Stuart Bolton. A finite difference approach for predicting acoustic behavior of the poro-elastic particle stacks. *INTER-NOISE and NOISE-CON Congress and Conference Proceedings*, NoiseCon22, Lexington, KY, Pages 1 - 976, pp. 350-361(12), 2022.